Technical Progress Report

Project Number DE-FG26-02NT41535
Development of All-Solid-State Sensors for Measurement of Nitric Oxide and Ammonia Concentrations by Optical Absorption in Particle-Laden Combustion Exhaust Streams

October 1, 2002 – December 31, 2006

Jerald A. Caton, and Kalyan Annamalai, Department of Mechanical Engineering, Texas A&M University, College Station, TX 77843-3123
Robert P. Lucht, School of Mechanical Engineering, Purdue University, West Lafayette, IN 47907-2088

ABSTRACT

An all-solid-state continuous-wave (cw) laser system for ultraviolet absorption measurements of the nitric oxide (NO) molecule has been developed and demonstrated. For the NO sensor, 250 nW of tunable cw ultraviolet radiation is produced by sum-frequency-mixing of 532-nm radiation from a diode-pumped Nd:YAG laser and tunable 395-nm radiation from an external cavity diode laser (ECDL). The sum-frequency-mixing process occurs in a beta-barium borate crystal. The nitric oxide absorption measurements are performed by tuning the ECDL and scanning the sum-frequency-mixed radiation over strong nitric oxide absorption lines near 226 nm.

In Year 1 of the research, the nitric oxide sensor was used for measurements in the exhaust of a coal-fired laboratory combustion facility. The Texas A&M University boiler burner facility is a 30 kW (100,000 Btu/hr) downward-fired furnace with a steel shell encasing ceramic insulation. Measurements of nitric oxide concentration in the exhaust stream were performed after modification of the facility for laser based NOx diagnostics. The diode-laser-based ultraviolet absorption measurements were successful even when the beam was severely attenuated by particulate in the exhaust stream and window fouling. Single-laser-sweep measurements were demonstrated with an effective time resolution of 100 msec, limited at this time by the scan rate of our mechanically tuned ECDL system.

In Year 2, the Toptica ECDL in the original system was replaced with a Sacher Lasers ECDL. The mode-hop-free tuning range and tuning rate of the Toptica ECDL were 25 GHz and a few Hz, respectively. The mode-hop-free tuning range and tuning rate of the Sacher Lasers ECDL were 90 GHz and a few hundred Hz, respectively. The Sacher Lasers ECDL thus allows us to scan over the entire NO absorption line and to determine the absorption baseline with increased accuracy and precision. The increased tuning rate is an advantage in that data can be acquired much more rapidly and the absorption

measurements are less susceptible to the effects of transient fluctuations in the properties of the coal combustor exhaust stream. Gas cell measurements were performed using the NO sensor with the new ECDL, and a few spectra were acquired from the coal exhaust stream. However, the laser diode in the new ECDL failed during the coal combustor tests. In Year 3, however, we obtained a new GaN laser diode for our ECDL system, installed it, and completed an extensive series of measurements in the Texas A&M coal-fired laboratory combustion facility. The combustor was operated with coal and coal/biomass as fuels, with and without reburn, and with and without ammonia injection. Several different fuel equivalence ratios were investigated for each operating condition.

TABLE OF CONTENTS

INTRODUCTION

Increasing concern over the environmental impact of combustion emissions have brought about many new governmental regulations in recent years. Besides high sensitivity, diode-laser-based sensors also offer non-intrusive and potentially continuous, real-time measurements of these gases. With these attributes, diode-laser-based sensors are ideally suited to be incorporated into control systems to optimize combustion processes and minimize emissions. Much work has been done in developing these types of sensors, but much less work has been done to demonstrate that this technology can be applied in realistic combustion environments.

In this final report we discuss the application of a diode-laser-based sensor for ultraviolet absorption measurements of nitric oxide in a particle-laden exhaust flow from a laboratory-scale coal combustor. In Year 2, a new ECDL was incorporated into our NO sensor system to increase the accuracy and precision of the measurements and to make the measurements even less sensitive to the effects of broadband attenuation. Initial measurements with improved sensor were very encouraging, but the 395-nm laser diode failed during the course of the first set of measurements in the coal exhaust stream. In Year 3 and the no-cost extension period, the 395-nm laser diode was replaced and the NO sensor was used to perform an extensive series of measurements in the Texas A&M coal-fired combustion facility.

EXPERIMENTAL APPARATUS

Diode-Laser-Based Nitric Oxide Sensor

The nitric oxide sensor utilizes the absorption of ultraviolet (UV) radiation near 226.8 nm by NO. A schematic diagram of the NO sensor is shown in Fig. 1. In the spectral region near 226 nm, the NO transitions are very strong and there is little interference from other molecules. UV radiation at this wavelength is generated by sum frequency mixing (SFM) the 10-mW output of an external-cavity diode laser (ECDL) at 395-nm with the 115-mW output of a frequency doubled, diode-pumped Nd:YAG laser at 532.299 nm (vacuum) in a beta-barium-borate (BBO) crystal. Approximately 250 nW of UV is generated in the SFM process. The UV beam is split into a signal and reference beam using a 50-50 beamsplitter. The reference beam is sent directly to a detector while the signal beam is directed through the combustion exhaust stream and then to a detector. Both beams are detected using solar blind photomultiplier tubes (PMTs). Interference filters centered at 228 nm are used to block the fundamental beams as well as any flame emission (which was not a problem in the experiments discussed here).

Absorption spectra are acquired by tuning the wavelength of the 395-nm ECDL so that the wavelength of the ultraviolet beam is tuned over NO absorption lines to produce a fully resolved absorption spectrum. The signal and reference traces from the solar-blind photomultiplier tubes, the output of a 2-GHz free-spectral-range (FSR) spectrum analyzer, and the ramp voltage applied to the grating piezoelectric crystal are acquired as the ECDL frequency is scanned. The mode-hop-free tuning range of the 395-nm ECDL used in the Year 1 experiments was 25 GHz. By controlling the diode laser current as we tuned the ECDL grating, we were able to obtain a mode-hop-free tuning range of almost 90 GHz with the Sacher Lasers ECDL, over a factor of three better than with the Toptica ECDL. After the 395-nm diode was replaced in Year 3, we were able to obtain approximately 60 GHz of mode-hop-free tuning; the performance was degraded slightly because the diode was from a different vendor. The increased mode-hop-free tuning range of the 395-nm ECDL has improves the accuracy and precision of our NO absorption measurements by minimizing any uncertainties in determining the unattenuated baseline for the NO spectral lines.

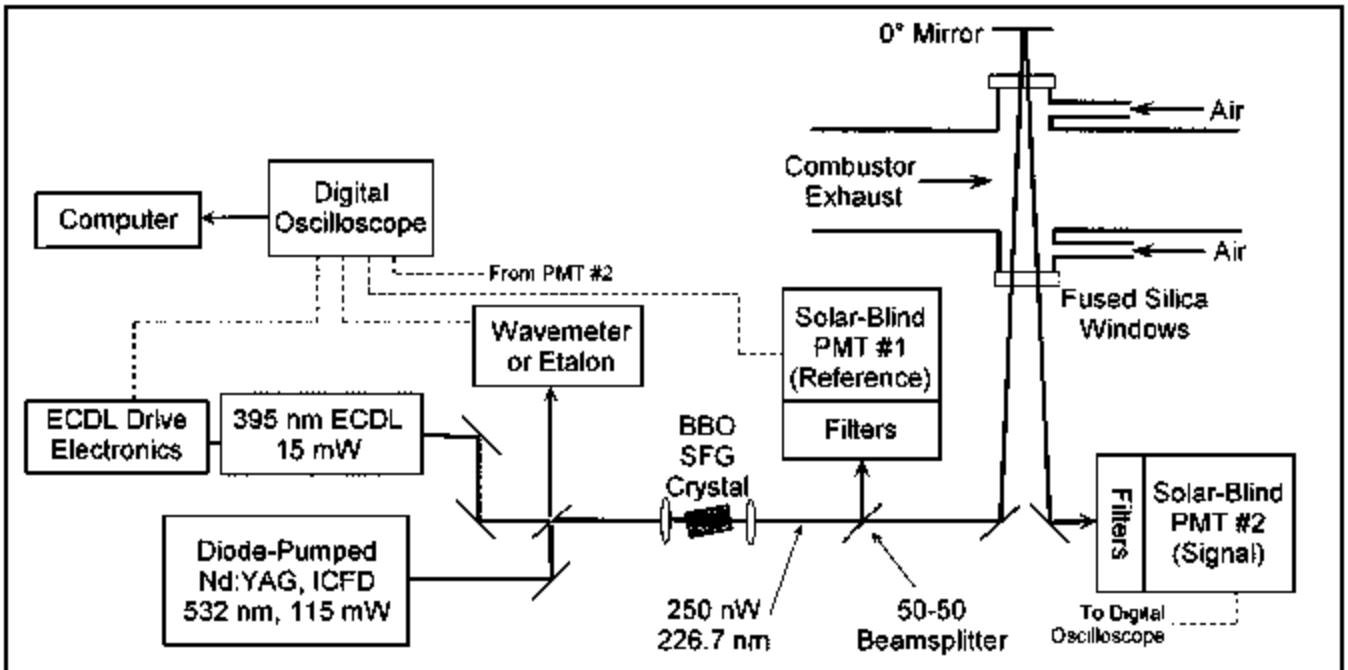

Fig. 1. Schematic diagram of the nitric oxide sensor measurements in the coal-particle-laden combustion exhaust stream.

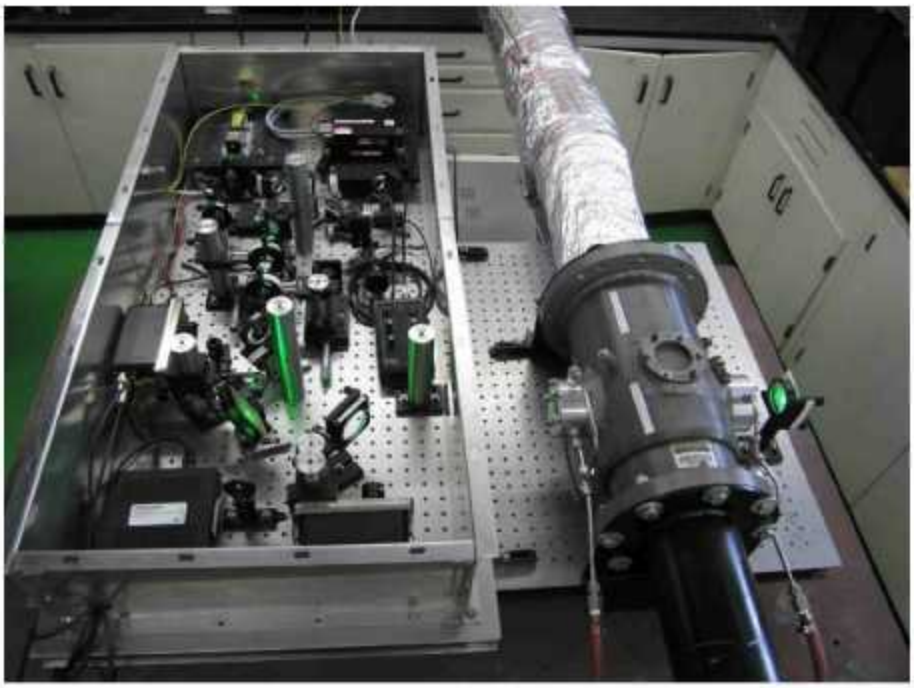

Fig. 4. Photograph of the NO sensor assembly (top) and the optical access chamber for the coal exhaust stream (bottom).

Coal Combustion Facility

A fully instrumented 100,000 BTU/hr (30 kW) boiler burner facility is available for sensor testing experiments. This facility can be fired with gaseous fuels, coal, biomass, and coal:biomass blends (Frazzitta et al., 1999; Annamalai et al., 2003; Sweeten et al., 2003). We have the capability of performing probe sampling emission measurements of NO, O_2, SO_2, and CO. The production of NO_x from coal:biomass combustion has been investigated extensively in previous experiments with this system.

The Texas A&M combustor provides an ideal device for development and testing of new sensor systems. The system is fairly small and inexpensive to operate but allows us to test the performance of the sensor under conditions very similar to those in an actual fossil fuel power plant. Parameters to be varied in the combustor for the sensor tests include equivalence ratio, furnace load, reburn fraction, and particulate loading in the exhaust stream.

The laboratory room next to the combustor facility has been converted to a sensor laboratory as part of the research activities connected with the University Coal Research program grant. The exhaust from the coal/biomass facility is being redirected through the sensor laboratory for measurements in the combustion exhaust. The level of particulate loading in the combustor exhaust stream can be controlled by varying the cooling water flow just upstream of the exhaust exit of the combustor (an additional water spray apparatus will be located downstream of the sensor to ensure that particulates are not exhausted to the atmosphere). The burner facility is built in sections. For future planned measurements in the primary combustion and reburn zones of the combustor, the appropriate sections of the combustor will be modified for optical access.

A new optical chamber was fabricated and installed during Project Year 2 and is illustrated in Fig. 2. Window assemblies with air flow directed across the windows to prevent fouling were designed and installed. The optical chamber is fitted with holes for insertion of physical probes for extracting samples for NOx measurement. The NOx concentrations in ppm are measured on dry basis (with water vapor removed by desiccant) using ENERAC 3000 E gas analyzer which uses electrochemical cells for measuring NO and NO_2 separately; typically NO_2 is very low and of the order of 2 ppm. Thus NO_x (NO + NO_2) is reported as NO.

RESULTS

The results of the NO sensor measurements in the coal exhaust stream are described in detail in a paper that has been accepted for publication by Applied Optics and is currently in press (Anderson et al., 2007). A reprint version of that paper is included as an attachment to this progess report.

REFERENCES

T. N. Anderson, R. P. Lucht, S. Priyadarsan, K. Annamalai, and J. A. Caton, "In-situ Measurements of Nitric Oxide in Coal-Combustion Exhaust Using a Sensor Based on a Widely-Tunable External Cavity GaN Diode Laser," *Applied Optics*, accepted for publication (2007).

K. Annamalai, B. Thien, and J. Sweeten (2003), "Co-Firing of Coal and Cattle Feedlot Biomass (FB) Fuels Part II: Performance Results from 100,000 BTU/Hr Laboratory Scale Boiler Burner," Fuel **82**, 1183-1193.

S. Frazzitta, K. Annamalai, and J. Sweeten (1999), "Performance of a Burner with Coal and Coal: Feedlot manure Blends," Journal of Propulsion and Power **15**, 181-186.

S. F. Hanna, R. Barron-Jimenez, T. N. Anderson, R. P. Lucht, J. A. Caton, and T. Walther (2002), "Diode-Laser-Based Ultraviolet Absorption Sensor for Nitric Oxide," Applied Physics B **75**, 113-117.

J. M. Sweeten, K. Annamalai, B. Thien, and L. McDonald (2003), "Co-Firing of Coal and Cattle Feedlot Biomass (FB) Fuels, Part I: Feedlot Biomass (Cattle Manure) Fuel Quality and Characteristics," Fuel **82**, 1167-1182.

In situ measurements of nitric oxide in coal-combustion exhaust using a sensor based on a widely-tunable external-cavity GaN diode laser

Thomas N. Anderson[1] and Robert P. Lucht

School of Mechanical Engineering, Purdue University

585 Purdue Mall, West Lafayette, Indiana 47907-2088

lucht@purdue.edu

Soyuz Priyadarsan[2], Kalyan Annamalai, and Jerald A. Caton

Mechanical Engineering Department, Texas A&M University

3123 TAMU, College Station, Texas 77843-3123

[1]Present address: ExxonMobil Upstream Research Company, P.O. Box 2189, Houston, TX 77252-2189

[2]Deceased

A diode-laser-based sensor has been developed to measure nitric oxide mole fractions using absorption spectroscopy. The sensor is based on sum-frequency mixing of a 395-nm external-cavity diode laser (ECDL) and a 532-nm laser in a beta-barium-borate crystal. Using a new tuning scheme, the GaN ECDL wavelength was modulated over 90 GHz without mode hops. The sensor was applied for measurements of NO mole fraction in the exhaust of a laboratory-scale, 30-kW$_t$ coal-fired boiler-burner. Absorption measurements were successfully performed despite severe attenuation by scattering from ash particles in the exhaust stream and on the exhaust-section windows. A detection limit (1σ) of 4.5 ppm-m/$\sqrt{\text{Hz}}$ at 700 K was demonstrated in coal combustion exhaust at a maximum detection rate of 5 Hz.

OCIS codes: 300.1030, 300.6260, 300.6540, 280.1120, 120.1740, 140.2020.

1. Introduction

Nitrogen oxides (NO_x) have been linked to many detrimental human health and environmental effects including ground-level ozone (smog), acid rain, global warming, and water-quality deterioration. Nitric oxide (NO) generated during combustion processes is the major source of NO_x in the atmosphere, and a large fraction of these NO emissions result from fuel combustion for electric-power generation. In particular, coal combustion generates high levels of NO emissions, contributing roughly one quarter

of the anthropogenic NO_x into the atmosphere annually.[1] In response to recent governmental regulations, much research has been performed to understand and reduce the emissions of NO from coal-fired combustion systems.[2–7] This research is becoming increasingly important as coal becomes a more important source of fuel due to its low cost, wide availability, and large U.S. reserves.

To support the ongoing research on NO formation and reduction in coal-combustion systems, new sensor technology is required to measure NO concentration in coal combustors. In addition, sensor technology is important for enabling new research directions such as real-time combustion control for reducing emissions.[8] Diode-laser-based sensors are frequently being applied for measuring pollutant concentrations in industrial combustors.[9–14] These sensors provide a non-intrusive method for measuring absolute species concentrations *in situ* in such harsh combustion environments. The fast, continuous, path-averaged concentration measurements available with these sensors are ideal for characterizing combustion conditions to optimize the combustion process and minimize emissions. Diode-laser-based sensors are rugged enough to survive the environments surrounding industrial combustors,[9–14] and a sensor for CO, H_2O, and temperature has even been demonstrated in a full-size coal-fired power plant.[11]

To our knowledge, no diode-laser-based sensors have been demonstrated for measuring NO in coal-combustion applications. In part, the lack of sensors is due to the difficulty of addressing NO transitions with available diode laser technology.

Previous sensors have been limited to the infrared (IR) spectral regions at 1.8, 2.65, and 5.3 μm where the fundamental outputs of commercial lasers overlap with NO transitions, as shown in Fig. 1.[15–26] Unfortunately, there is significant interference from absorption by water vapor since these same spectral regions coincide with strong water vapor transitions, also shown in Fig. 1. Interference with other species such as CO_2 is also a potential problem with the IR measurements. Sensors based on lead-salt and quantum-cascade lasers have been used with some success in the mid-IR between 5.2 and 5.4 μm,[20–26] but cryogenically-cooled detectors, sparse laser availability, and complicated laser-control requirements have hampered the application of these systems to realistic combustors.

By contrast, detection of NO in the ultraviolet (UV) spectral region offers significantly stronger line strengths and reduced interference from absorption by other species (see Fig. 1). Koplow *et al.* first demonstrated a diode-laser-based system for detecting NO in the UV,[29] but the system was based on a tapered amplifier that is no longer available. The recent commercialization of GaN diode lasers emitting radiation around 400 nm has enabled us to develop a diode-laser system that utilizes sum-frequency mixing (SFM) to generate tunable, narrowband UV radiation in a compact package for absorption spectroscopy of NO.[30] This diode-laser-based sensor is rugged enough to perform *in situ* measurements of NO in practical combustors, and we have previously applied the sensor for measurements of NO in the exhaust of a gas-turbine engine.[31]

In this paper, we describe the application of our UV diode-laser-based sensor for *in situ* measurements of NO in the exhaust of a laboratory-scale, coal-fired boiler burner. We have incorporated a new tunable laser into the sensor system to increase the mode-hop-free tuning range of the UV radiation. By modulating the commercially available GaN external-cavity diode laser (ECDL) with a new control scheme, we have achieved a mode-hop-free tuning range of 90 GHz for the UV laser radiation. This range is over three times as large as our previous laser system, enabling us to scan over an entire NO transition in the coal-combustion exhaust at atmospheric pressure. The increased mode-hop-free tuning range improves the accuracy of the spectral fitting procedure so that we can discriminate against severe broadband attenuation by scattering from coal and ash particles in the exhaust stream. The accuracy of the diode-laser-based sensor measurements were verified by independent measurements using a commercial NO electrochemical sensor with extractive sampling. The successful measurements of NO in coal-combustion exhaust reported in this paper demonstrate the utility of this diode-laser-based sensor system for facilitating research on NO emissions reduction in actual coal-fired combustors.

2. Widely-Tunable External-Cavity GaN Diode Laser

Ultraviolet radiation for the NO sensor is generated by sum-frequency mixing the output of a tunable 395-nm external-cavity GaN diode laser with the output of a 532-nm compact, diode-pumped, intracavity-frequency-doubled Nd:YAG laser in a

beta-barium borate (β-BBO) crystal.[30,31] The wavelength of the generated UV radiation is scanned across the NO transition by modulating the wavelength of the ECDL. In the previous version of the sensor, we used a commercially available 395-nm ECDL (Toptica Photonics) which had a 24-GHz mode-hop-free tuning range using the built-in scanning module in the laser controller.[30,31] The resulting tuning range of the UV radiation is also 24 GHz, and therefore we could not scan completely over an absorption feature of NO at atmospheric pressure. In general, the absorption lineshapes for NO are known well enough that the spectral fits were accurate despite the narrow tuning range, and thus the NO concentrations measured with the sensor were accurate. However, a wider mode-hop-free tuning range provides more spectral information to improve the accuracy of the spectral fits, especially in environments with severe broadband attenuation of the UV beam. In this section, we describe a modified control scheme to increase the mode-hop-free tuning range of a commercial GaN ECDL to improve the accuracy of the diode-laser-based NO sensor measurements.

Two groups have recently published innovations for extending the mode-hop-free tuning range of external-cavity GaN diode lasers. Before discussing these innovations, the basic operation of ECDLs will be reviewed. The simplest configuration for an ECDL is shown in Fig. 2, where the diffraction grating is mounted in the Littrow configuration. In this configuration, the first-order diffracted beam from the diffraction grating is directed back into the laser diode as feedback. A laser cavity is formed between the back facet of the laser diode and the diffraction grating (external-cavity

modes), as well as between the front and back facets of the laser diode chip (Fabry-Perot, or FP modes). Gain (and hence laser emission) occurs only when longitudinal modes of the external-cavity and the laser diode overlap within the peak of the feedback profile of the diffraction grating.

To modulate the output wavelength of the ECDL, both the angle of the grating and the length of the external cavity must be changed simultaneously so that the change in feedback wavelength from the grating is equal to the change in wavelength due to the cavity length change. This rotation/extension is typically achieved by mounting the grating on a lever arm that pivots about a carefully chosen point, as shown in Fig. 2, so that both grating rotation and cavity-length extension occur when the piezoelectric actuator is changed. For current commercial GaN ECDLs, this modulation results in roughly 8 GHz of tuning before the longitudinal mode of the external cavity jumps to a different FP mode, commonly called a mode-hop.[32] If the injection current of the laser diode is also modulated concurrently with the grating angle, then the FP modes will also change in wavelength, and the output wavelength of the ECDL can be scanned over a much wider range without mode hops.

This "current-compensation" technique is commonly employed in commercial ECDLs, including the GaN ECDL used in the previous version of our NO sensor. Other groups have demonstrated similar mode-hop-free tuning ranges around 20 GHz with similar ECDLs.[33] In these previous ECDLs, the GaN laser diode facets have not been anti-reflection (AR) coated. However, Hildebrandt *et al.* have achieved a

mode-hop-free tuning range of over 50 GHz with the same configuration and current compensation by using an AR-coated laser diode.[32] As shown in Fig. 2, the front facet of a GaN laser diode was coated with a high-quality anti-reflection (AR) coating, and the laser diode was used in an external cavity in the Littrow configuration. As will be discussed, the maximum mode-hop-free tuning range for this ECDL was due to a mismatch between the FP mode and the external-cavity mode after 50 GHz of tuning.

Hult *et al.* have also demonstrated an innovative approach to increase the mode-hop-free tuning range of GaN diode lasers in a Littrow external cavity configuration. They developed a new mount for the diffraction-grating with multiple piezoactuators to adjust the cavity length and grating angle independently.[35] By carefully synchronizing the adjustment of the grating angle, the external cavity length, and the diode injection current, they were able to achieve a mode-hop-free tuning range of 93 GHz for a non-AR-coated GaN diode laser at 410 nm. For this ECDL, the limiting factor in the mode-hop-free tuning range was the current limits for the diode laser, since the current compensation resulted in a variation of the injection current from the maximum to below the threshold current.

Although the system developed by Hult *et al.* provides an excellent mode-hop-free tuning range even without AR-coating the laser diode, it is not commercially available. By contrast, the AR-coated GaN laser diodes described in Hildebrandt *et al.* are now commercially available through Sacher Lasertechnik in the Littrow configuration.[34] Using this ECDL as purchased, we have been able to achieve a mode-hop-free tuning

range of 90 GHz by modifying the modulation signals to more carefully match the change in external-cavity mode with the FP mode while tuning.

The 395-nm ECDL (TEC-100-405-15) was purchased from Sacher Lasertechnik along with the controller (MLD-1000) and an analog modulation module (PI-1000-MD). The analog modulation module allows for the injection current for the diode to be externally controlled via a voltage (V_{current}) applied to the BNC connector on the front panel of the module. The laser controller includes the piezo amplifier, which allows the piezoelectric actuator to be externally controlled through a voltage (V_{piezo}) applied to another BNC connector. Through these two inputs, we can control the grating angle and external cavity length (simultaneously with the piezo) and the injection current of the laser diode. The grating angle and external cavity length cannot be changed independently of each other since the grating was mounted on a lever arm as shown in Fig. 2. Nonetheless, a large mode-hop-free tuning range was still obtained because we carefully overlapped the active FP and external-cavity modes by our modulation technique. Hult *et al.* also noted the insensitivity of the mode-hop-free tuning range on grating angle, mainly because of the comparatively large bandwidth of the diffraction grating.[35]

Modulation signals for controlling the ECDL were generated using a computer with an analog input/output card (National Instruments, Inc.; PCI-6251) and LabVIEW software. This data acquisition (DAQ) system was also used to record the signals from the photodetectors in the remainder of the sensor, as described in the next

section. A single cycle of each modulation waveform was calculated in a LabVIEW program and then applied at a specified rate to the ECDL controller via the analog input/output card. For controlling the piezoelectric actuator, a triangle-wave function was generated with an amplitude $V_{\text{piezo,max}}$ according to the equation

$$V_{\text{piezo}} = V_{\text{piezo,max}} \left(\frac{4}{N} i - 1 \right), \tag{1}$$

where N is the number of points in a single cycle of the waveform and i varies from 0 to $N/2$ to generate the first half of the waveform. The second half of the waveform was generated in LabVIEW by inverting the array and concatenating to the end of the original array.

In the typical implementation of the current-compensation technique, the control signal applied to the injection current (V_{current}) has the same shape as the piezo signal (i.e., a triangle-wave function), but it is multiplied by a negative fraction to reduce the amplitude and shift the waveform 180° out of phase from the piezo signal. However, this method does not completely preserve the overlap of the active external-cavity mode and FP mode over the entire scan range, which limits the mode-hop-free tuning range. We found that by adding a slight amount of curvature to the control signal, V_{current}, the overlap is better preserved and a larger mode-hop-free tuning range is achieved. A second-order polynomial was used to calculate the control signal for modulating the injection-current according to the equation

$$V_{\text{current}} = -V_{\text{piezo,max}} \cdot \alpha \left[\left(\frac{4}{N} - \frac{\beta N}{2} \right) i + \beta i^2 - 1 \right]. \quad (2)$$

Here, the factor α is used to adjust the amplitude of the waveform and β is used to adjust the curvature of the waveform (through the quadratic term in the polynomial). As with the piezo control signal, this equation was used to calculate the first half of the current control waveform and the second half was generated by manipulating the array in LabVIEW. A single cycle of both waveforms is shown in Fig. 3 for typical values of the variables.

The values for the three variables, $V_{\text{piezo,max}}$, α, and β, were determined experimentally by varying each while monitoring the tuning of the ECDL with a spectrum analyzer (Burleigh; SAPlus). *The tuning range of the ECDL was optimized systematically using the following method. To begin, the values for α and β were set to zero and the piezo-voltage amplitude ($V_{\text{piezo,max}}$) was set to a small value so that only a small mode-hop-free tuning range (< 10 GHz) was observed. Then, the piezo-voltage amplitude was increased until multi-mode output was observed at the beginning or end of the scan range. To correct these mode hops near the edges of the scan, the current compensation (α) was adjusted. Once single-mode operation was achieved over the entire scan range, the piezo-voltage amplitude was increased again and the procedure was repeated. Typically, up to 50 GHz of mode-hop-free tuning range could be obtained without using the curvature (β). Once the scan range exceeded 50 GHz, then both α*

and β were adjusted to achieve mode-hop-free tuning over the entire scan.

In most instances, the tuning range was limited by the injection current, in which case the output power of the laser drops to zero when the current nears the threshold current. At this point, the laser tuning range was optimized and experiments were started. The Sacher ECDL controller has a built-in gain of 10, so we typically applied a piezo control signal with an amplitude of 1 to 1.5 V, corresponding to an actual voltage of ± 10 to 15 V at the piezoelectric crystal. For our GaN ECDL, the optimum values were found to be $V_{\text{piezo,max}} = 1.1$ V, $\alpha = 0.2150$, and $\beta = 0.6 \times 10^{-7}$. With settings around those values, we achieved a mode-hop-free tuning range of up to 90 GHz with the ECDL, as demonstrated in Fig. 4.

The 90-GHz mode-hop-free tuning range achieved using the new modulation scheme is a significant improvement over the 20 GHz mode-hop-free tuning range listed in the manufacturer's specifications.[34] Our large mode-hop-free tuning range is also an improvement over the 50 GHz demonstrated by Hildebrandt *et al.* for the same laser system at 410 nm.[32] When we modulate our ECDL without curvature (i.e., $\beta = 0$), the largest achievable mode-hop-free tuning range is also approximately 50 GHz, indicating the significance of the curvature term β in our current-compensation technique.

We demonstrated the same mode-hop-free tuning range as was achieved by Hult *et al.* for a non-AR-coated 410-nm ECDL using their custom external cavity design.[35] With the approach described here, we can achieve identical tuning performance without having to build a custom ECDL. Instead, a commercial ECDL system can be

used in conjunction with a simple DAQ system which, in most systems, is already required for recording photodetector signals. This new approach can be used to improve the mode-hop-free tuning range in a variety of systems already being used for various spectroscopic applications. Many such applications have been limited to atomic species with narrow linewidths such as potassium,[36] lead,[36] aluminum,[37] and gallium.[38] Measurements of broader atomic species such as NO_2 have been proposed using frequency-modulation spectroscopy once a GaN ECDL is available with a 50 GHz continuous mode-hop-free tuning range.[36] In the remainder of this paper, we describe the application of the sensor based on this widely-tunable ECDL for measurements of NO in the exhaust stream of a coal-fired combustor to demonstrate the utility of the improved mode-hop-free tuning range attained using our new modulation scheme.

3. Experimental System

3.A. Diode-Laser-Based Sensor

A diagram of the complete diode-laser-based sensor system is shown in Fig. 5. As mentioned in the previous section, UV radiation near 226.8 nm was generated by sum-frequency mixing (SFM) the 395-nm ECDL output with the 532-nm laser output in a β-BBO crystal. Details on the optical components and the alignment procedure can be found in our previous papers,[30,31] but the main features are discussed here. Beams from both lasers were overlapped and focused into the BBO crystal where approximately 130 nW of UV was generated for laser powers of 85 mW (532 nm)

and 21.5 mW (395 nm). The UV power was estimated from the current generated by the photomultiplier tube (PMT; Hamamatsu, R7154) using the specified sensitivity of the PMT after accounting for losses from optical filters.

The generated UV beam was recollimated with a fused-silica lens and then split into two beams using a 50/50 beamsplitter. The reflected beam (reference beam) was directed immediately through optical filters and onto a PMT to monitor the change in laser power during modulation. The transmitted beam (signal beam) was directed through the combustion-exhaust stream and onto a second PMT located behind optical filters. For both PMTs, narrowband interference filters (Andover Corp.; 228FS10-25) centered at 228 nm were used to block the fundamental beams and room lights; neutral density (ND) filters were also used to prevent saturation and maintain linearity of the PMTs. As discussed in Anderson *et al.*,[31] a cylindrical lens was placed after the beamsplitter to compensate for horizontal divergence of the UV beam due to the SFM process. The entire optical system was constructed on a 61×122 cm optical breadboard and enclosed in an aluminum housing for protection and thermal stability. It should be noted that the sensor size can be significantly reduced by careful component selection and placement, and we have constructed sensors as small as 46×46 cm for a similar system for detecting atomic mercury.[39]

Prior to the start of the experiments, the ECDL wavelength was tuned to 395.231 nm (vacuum) so that, when mixed with the CrystaLaser at 532.301 nm (vacuum), the generated UV radiation was in resonance with the $P_2(10)$ and $P_{12}(10)$ overlapped

transitions at 44087.75 and 44087.78 cm^{-1} in the (v''=0,v'=0) band of the $A^2\Sigma^+$-$X^2\Pi$ electronic transition of NO (see Ref. 31). The wavelength of the UV radiation was tuned back and forth across this transition by modulating the ECDL as described in Section 2. Approximately 70 GHz of mode-hop-free tuning range was typically achieved with a scan rate of no more than 20 Hz. Above this scan rate, the tuning range began to degrade due to mechanical vibrations and hysteresis of the piezo. This mode-hop-free tuning range is smaller than the 90 GHz demonstrated in Section 2 because the diode was replaced. *The newer diode had a longer, narrower active area, and therefore it was more difficult to maintain the alignment of the feedback from the grating into the laser diode over a large change in grating angle, thereby reducing the mode-hop-free tuning range.* Nonetheless, the 70-GHz mode-hop-free tuning range is almost three times as large as our previous system and significantly improves the results (see Section 4).

A spectrum analyzer with a 2-GHz free-spectral range was used to monitor the frequency tuning of the ECDL, as shown in Fig. 5. Signals from the spectrum analyzer and both PMTs were recorded on the computer via the analog input/output card. Photocurrents from the PMTs were detected across 100-kΩ resistors prior to digitization. We recorded data over 40 complete sweeps of the laser-frequency, and the amount of averaging was determined in post-processing. Alternately, all signals were recorded with a digital oscilloscope (with 1 MΩ impedance) and transferred to the computer via a GPIB interface, as described in Anderson *et al.*[31] When the oscil-

loscope was used, averaging was performed in real-time, summing over 8 to 256 laser sweeps.

Data were processed off-line according to the procedure described in Anderson *et al.*[31] Before processing, raw data were also filtered in software with a 10-kHz low-pass filter to reduce random noise. Broadband attenuation was corrected by scaling the normalized transmission until the theoretical and experimental absorption lineshapes agreed over the entire spectrum, as discussed in Anderson *et al.*[31] The effectiveness of the transmission correction is discussed further in Section 4. NO mole fractions and collision widths were varied in a least-squares fit to the experimental spectra while the pressure, temperature, and path length were fixed at values measured independently.

3.B. Coal-Fired Boiler Burner Facility

Measurements of NO mole fraction with the diode-laser-based sensor were performed in the exhaust of a 30 kW_t boiler burner that was fired with pulverized coal or a coal/biomass blend. The facility at Texas A&M University is a downward-fired furnace consisting of nine refractory-lined steel sections, as shown in Fig. 6. Further details of the facility and instrumentation are given in Annamalai *et al.* and Frazzitta *et al.*[40–42] For these experiments, a mixture of propane, ammonia, and preheated air was fired in the main burner at the top of furnace to generate 500 ppm of NO in the primary zone to simulate the conditions in an actual coal-fired power plant burner.[40] After the primary zone, a mixture of air and pulverized coal or coal/biomass blend

was injected into the furnace to study the NO reduction through a process called "reburn".[4,40,43] Approximately 70% of the thermal throughput was generated in the primary burner while the remaining 30% was supplied by the reburn fuel. Combustion continued downward through the remainder of the furnace, and the products exited through the exhaust duct.

Combustion exhaust gases were routed into an adjacent room (the sensor room) through approximately 10 m of insulated rigid ducting and into the exhaust test section for sensor measurements. As shown in Fig. 5, the exhaust test section was a modified portion of the exhaust duct with optical access for the UV beam from the NO sensor. Removable window flanges were attached to the duct so that the windows could be cleaned periodically to remove coal and ash buildup. The window flanges were also equipped with three ports for flowing air onto the inside surface of the windows to slow the buildup of coal and ash particles. Uncoated fused-silica windows were used, since the high temperatures encountered and frequent cleaning required would damage special optical coatings. The optical path length between the two windows was 27 cm, so the total path length of the UV beam through the exhaust stream was 54 cm with the two-pass arrangement.

A K-type thermocouple was placed in the exhaust duct approximately 1 m upstream of the test section to measure the exhaust gas temperature. Spectral fits for all data were calculated based on the temperatures measured at this location. The NO mole fraction in the exhaust was also independently measured using an electrochem-

ical (EC) sensor (Enerac; Model 3000E) that was calibrated before the experiments with 1000 ppm NO. The reported accuracy of the sensor was 2%. *The EC sensor could also be used to measure NO_x to determine if there was any conversion of NO.* Exhaust gas was sampled from one of five probes located across the exhaust test section and analyzed with the EC sensor to determine the NO distribution along the UV-beam path. The purge air at the windows diluted the NO mole fraction in the exhaust gas near the windows, so knowledge of the actual NO distribution was required for comparison of the diode-laser-sensor measurements to the EC-sensor measurements.

4. Coal-Combustion Exhaust Measurements

Prior to the measurements using the NO sensor with the new ECDL, measurements of NO were performed in the coal-combustion exhaust stream exhaust using the previous ECDL.[44] A representative absorption spectrum from the earlier experiments is shown in Fig. 7a for comparison with the absorption spectrum in Fig. 7b acquired using the new widely-tunable ECDL. Both spectra were acquired *in situ* in the exhaust stream. This figure demonstrates the significant improvement in mode-hop-free tuning range achieved by using the new ECDL and modulation scheme described in Section 2. In Fig. 7, it is evident that the increased spectral information collected with the new sensor system increases the accuracy and reliability of the spectral fits.

The increased mode-hop-free tuning range is especially important for measurements in media such as coal-combustion exhaust, where there is severe broadband attenua-

tion of the UV beam due to particulate scattering and absorption by other species. Typically, this broadband attenuation is corrected with a transmission scaling factor that is determined from an off-resonant portion of the spectrum where attenuation is not due to absorption by NO. However, there is no off-resonant baseline available within the tuning range of the sensor (as seen in Fig. 7), so we must use the shape of the absorption spectrum to determine the transmission scaling factor. Since we can now scan over an entire NO absorption lineshape with the wide mode-hop-free tuning range, we simply allow this parameter to vary during the spectral fitting and therefore any broadband attenuation is automatically corrected using our processing software. *We have demonstrated the accuracy of a similar transmission correction procedure in a similar sensor for atomic mercury.*[39] *In addition, the validity of the transmission correction is demonstrated by the agreement between experimental and theoretical lineshapes and between diode-laser and EC-sensor measured NO mole fractions.*

In addition to correcting for the broadband attenuation during post-processing, we also made adjustments during the experiments to maintain a high signal-to-noise ratio (SNR) in the recorded spectra. Over the course of 2 hours during the experiments, the UV laser radiation transmitted through the exhaust test section was reduced by a factor of 40 due to the buildup of coal and ash particles on the windows. This fouling occurred even with the air purge on the windows. To compensate for the steadily decreasing transmission through the windows over the course of the experiments, we periodically reduced the optical density (OD) of the ND filters located in front of the

signal PMT (PMT#2 in Fig. 5). At the beginning of the experiments, the UV beam was attenuated by a factor of 100 with an ND filter with OD 2 before reaching the PMT. As the laser power dropped due to window fouling, we manually replaced this ND filter with lower OD filters so that we maintained a relatively constant UV power onto the PMT. Since the shot-noise limit is proportional to the square root of the laser power incident on the PMT, we therefore maintained (at least theoretically) a constant SNR throughout the experiments. Given that the UV laser beam is attenuated by a factor of 100 using ND filters at the start of the experiments, we can thus compensate for window-fouling that attenuates the UV beam by more than a factor of 100.

To examine the accuracy of the NO mole fractions determined from the spectral fits after the broadband-attenuation correction, we compared the diode-laser sensor measurements to measurements made with the EC sensor. To directly compare measurements from the two techniques, the path-averaged nature of the diode-laser-sensor measurements must be considered. Measurements with the EC sensor on gas sampled at three different locations across the exhaust test section are shown in Fig. 8. At the windows ($\pm$13.5 cm), the NO mole fraction was assumed to be 0 ppm because of the air purge. A fourth-order polynomial was fit to the measured data points, as shown in Fig. 8. Integrating over the NO distribution described by the polynomial, the path-averaged NO mole fraction was determined to be 162 ppm. An absorption spectrum acquired at the same time is shown in Fig. 9, and the measured NO mole

fraction is 169 ppm.

While the measurements from both the EC sensor and diode-laser sensor agree closely for this instance, we observed larger deviations for other conditions. We expect a difference between the two methods for two reasons. First, the fourth order polynomial is a very crude approximation of the actual NO distribution across the exhaust duct. Second, we have not accounted for the temperature distribution across the exhaust stream. Since room-temperature air was used for the window purge, the temperature across the beam path likely varied between room temperature and the peak exhaust temperature (typically 600-700 K). The line strength of the NO transition being studied decreases by a factor of 2 as the temperature increases from 300 K to 700 K. Thus, the NO near the windows should contribute more to the absorption lineshape. Since we do not know the exact temperature profile, we cannot quantitatively estimate the effect on the absorption lineshape. However, we believe that the effect on the absorption lineshape is minimal since the NO mole fraction drops to zero in these lower-temperature regions. Also, the flow rate of the air purge was quite low, so the low-temperature mixing region is confined closer to the windows which again limits the effect on the absorption lineshape. Some groups like Sanders et al.[46] *have attempted to determine spatial temperature and concentration gradients using diode-laser-based sensors, demonstrating that it is feasible to obtain useful information with diode-laser-based sensors in inhomogeneous flows. The measurements reported in this paper represent an initial step towards such a sensor by demonstrating that our UV*

system can be used in highly absorbing media, and the path-averaged measurements obtained with our system are reasonable based on independent measurements with the EC sensor.

It should be noted that the NO mole fractions were measured by the electrochemical sensor on a dry basis by removing the water vapor from the sampled gas before analysis. The diode-laser-based sensor measurements were on a wet basis since they were performed in situ *in the exhaust with water vapor present. The wet basis is estimated to be approximately 10 ppm lower than the dry basis measurements.[44] The mole fractions listed in all figures are not corrected for this difference. In addition, the EC sensor did not detect any difference between NO and NO_x, indicating that there was no conversion to NO_2 in the exhaust.*

As another check on the accuracy of the diode-laser-based sensor measurements, we can compare the measured widths of the absorption lineshapes with predictions from the literature. The line width for the Voigt profile is composed of the Doppler width and the collision width. The Doppler width was calculated using the code (see Ref. 31) based on the temperature measured by the thermocouple in the exhaust duct. The collision width was varied during the least-squares fit to match the experimental data. An example of a typical collision width is shown in Fig. 9, where the collision width is 0.367 cm^{-1}. Using expressions given in Anderson et al. *and references therein,[31] the collision width for NO can be estimated for a given exhaust composition and temperature. At the exhaust temperature, the predicted collision width for pure nitrogen is 0.31 cm^{-1}*

and for pure water vapor is 0.40 cm^{-1}. Thus, the collision width will be slightly larger than 0.31 cm^{-1} due to broadening by the water vapor and other molecules. In addition, the temperature is likely lower than the thermocouple measurement because of the purge air, and hence the collision widths for all species are slightly higher since the collision broadening coefficients are inversely proportional to temperature. Therefore, the predicted collision width lies near the measured collision width, demonstrating that the lineshapes recorded with the system are accurate and no instrumental broadening is present.

From the spectrum in Fig. 9 and similar spectra, the noise in the residual (experiment minus theory) is approximately 0.0064 for an averaging time of 5 seconds. This corresponds to a detection limit (1σ) of approximately 2 ppm in one meter of gas at 700 K. Normalized by the bandwidth, the detection limit was 4.5 ppm-m/$\sqrt{\text{Hz}}$. By reducing the number of spectra averaged, we can improve the time resolution of the diode-laser sensor for applications that need to measure faster NO fluctuations. As an example, Fig. 10 shows an absorption spectrum of NO acquired in 0.2 seconds with the diode-laser sensor. This spectrum represents an average of 8 sweeps of the laser frequency while scanning the ECDL at 20 Hz. It should be noted that single absorption spectra are obtained at 40 Hz since a complete cycle of the laser frequency generates two absorption spectra. Fig. 10 also shows the change in detected UV power as the GaN ECDL wavelength was scanned, indicating that the increased noise near the high-frequency end of all the spectra is due to low laser power. The noise in the

residual of Fig. 10 is approximately 0.034, which corresponds to a 1σ detection limit of 10 ppm-m in 700 K gas, or 4.5 ppm-m/$\sqrt{\text{Hz}}$.

The detection limits achieved during these experiments represent a slight improvement from our previous paper,[31] mainly because of reduction in digitization noise. However, the detection limit is still approximately one order of magnitude worse than the shot-noise limit for the system. The increase in noise above the shot noise limit is partly due to particle scattering in the exhaust and beam steering effects through the hot, turbulent flow in the exhaust duct. In comparison with other diode-laser-based systems, sensors based on QC lasers operating in the fundamental vibrational band near 5.26 μm have achieved detection limits of 0.2 ppm-m/$\sqrt{\text{Hz}}$ NO at 630 K.[26] Although NO transitions are four orders of magnitude weaker in the MIR than in the UV (see Fig. 1), the QC-laser-based sensors have much better signal-to-noise ratios because of the high peak powers of the QC lasers. By contrast, the PMTs in the UV laser system cannot accept more than 1 nW, so the best achievable detection limit with this UV system is several orders of magnitude worse than that of QC-laser-based systems. However, as improvements in laser and detector technology allow us to generate and utilize more UV power, then a UV sensor for NO could provide superior detection limits due to the strong NO transitions in the UV.

Measurements of NO in the coal-combustion exhaust were performed with both the diode-laser sensor and EC sensor to study the effect of fuel type and stoichiometry on NO reduction through reburn. As mentioned in Section 3.B, 500 ppm of NO was

generated in the primary zone of the furnace and either coal or coal/biomass were fired in the reburn section to reduce the NO emissions from the burner. Measurements of NO in the exhaust stream at the test section using both sensors are summarized in Fig. 11 for all conditions studied. It should be noted that the NO mole fractions in the exhaust test section are artificially diluted from the purge air on the windows, but the trends in the NO reduction are clear from the measurements. For the coal reburn cases, only the NO mole fraction at the center of the duct was measured with the EC sensor. Therefore, we assumed that the NO distribution followed that shown in Fig. 8, except the magnitude of the distribution was scaled to match the value measured with the EC sensor at the center of the duct. Using this approach, we estimated the path-averaged NO mole fractions from the EC sensor measurement at the center of the duct. The difference between the diode-laser measurements and this path-averaged EC sensor measurement in Fig. 11 for the coal cases is most likely due to this poor estimation of the actual NO distribution across the exhaust duct. However, both measurement techniques indicate a slight decrease in NO mole fraction in the exhaust for the higher equivalence ratio using coal as the reburn fuel.

Using a coal/biomass blend as the reburn fuel, the NO emitted from the burner is significantly lower than for using only coal, as shown in Fig. 11. For the biomass cases, the NO distribution was directly measured in the exhaust for each equivalence ratio. The path-averaged mole fractions measured with both the diode-laser sensor and the EC sensor agree closely for the Φ=1.2 case. The discrepancy in the Φ=1.0 case is

likely due to the estimated NO distributions or fluctuations in the NO mole fraction in the exhaust. We observed fluctuations of 20% in the NO mole fraction in the exhaust over the course of several seconds using the diode-laser sensor. Therefore, the different integration times of the diode-laser sensor and the EC sensor likely lead to different NO measurements. Nonetheless, both measurement techniques demonstrate the NO reduction capabilities of reburn with biomass, especially at a higher equivalence ratio, which has been observed previously by Annamalai and coworkers.[40] Annamalai *et al.* attributed this reduction to a lower O_2 concentration in the reburn section to reduce NO production and also to the formation of NH_3 from the biomass, which reacts with NO to form N_2.[41]

5. Conclusion

We report what is to our knowledge the first *in situ* measurements of NO in coal-combustion exhaust with a diode-laser-based sensor. The sensor was based on sum-frequency mixing of a 395-nm GaN ECDL with a 532-nm laser to generate tunable, narrowband UV radiation near 226.8 nm for absorption spectroscopy of NO. A new control scheme was developed to modulate a commercial GaN ECDL, and a mode-hop-free tuning range of 90 GHz was achieved. Using the widely-tunable GaN ECDL in the sensor system, the generated UV radiation was continuously scanned over an entire NO absorption lineshape at atmospheric pressure. The wide mode-hop-free tuning range allowed us to accurately discriminate against broadband attenuation

in the coal-combustion exhaust due to scattering from particulates in the exhaust stream and on the windows of the test section. NO measurements with the diode-laser sensor were successfully demonstrated even in the case of attenuation by a factor of 40. The accuracy of the diode-laser-sensor measurements was verified by comparison with measurements using extractive sampling and an electrochemical sensor. When the electrochemical sensor measurements were corrected for the NO spatial profile across the exhaust stream, measurements using both techniques were in reasonable agreement. The detection limit (1σ) of NO in the exhaust stream (at 700 K) was demonstrated to be approximately 4.5 ppm-m/$\sqrt{\text{Hz}}$ at a maximum detection rate of 5 Hz. Using the diode-laser-based sensor, the effect of reburn on NO reduction was studied in the laboratory-scale boiler burner. Combustion of a coal/biomass blend in the reburn zone was found to significantly reduce the NO mole fraction in the exhaust stream.

These experiments demonstrate methods for applying UV absorption in highly absorbing media, allowing the diode-laser-based NO sensor to be used successfully in particulate-laden combustion exhaust streams like those found in coal-combustion applications. Although the measurements cannot be considered absolute due to uncertainties in the path length and large inhomogeneities in the exhaust, the diode-laser-based sensor could still potentially be used to non-intrusively obtain a global measure of NO mole fraction in coal combustion systems in real time. Such capabilities could be valuable for studying overall NO reduction in coal combustors through combustion

modifications. In addition, unsteady combustion phenomena in coal-combustion systems could be studied with a fast laser system, as we have previously demonstrated with hydroxyl (OH) in a turbulent gas-turbine combustor.[45] *With the demonstrated 0.2-second time resolution and with further work towards online data analysis, this sensor could feasibly be incorporated into a combustion-control system to continuously monitor and control NO emissions from coal-fired power plants.*

This work was supported by a grant from the U.S. Department of Energy, University Coal Research Program, Award No. DE-FG26-02NT41535 (Dr. Richard J. Dunst, contract monitor). Thomas Anderson was supported by a National Science Foundation Graduate Research Fellowship.

References

1. U. S. Environmental Protection Agency, "National Air Quality and Emissions Trends Report: 2003 Special Studies Edition," EPA 454/R-03-005 (U. S. Environmental Protection Agency, Office of Air Quality and Standards, Research Triangle Park, N.C., 2003); www.epa.gov/air/airtrends/aqtrnd03.
2. J. M. Beer, "Combustion technology developments in power generation in response to environmental challenges," Prog. Energy Combust. Sci. **26,** 301-327 (2000).
3. A. Williams, M. Pourkashanian, and J. M. Jones, "Combustion of pulverised coal

and biomass," Prog. Energy Combust. Sci. **27,** 587-610 (2001).

4. L. D. Smoot, S. C. Hill, and H. Xu, "NO_x control through reburning," Prog. Energy Combust. Sci. **24,** 385-408 (1998).

5. A. Molina, E. G. Eddings, D. W. Pershing, and A. F. Sarofim, "Char nitrogen conversion: implications to emissions from coal-fired utility boilers," Prog. Energy Combust. Sci. **26,** 507-531 (2000).

6. S. C. Hill and L. D. Smoot, "Modeling of nitrogen oxides formation and destruction in combustion systems," Prog. Energy Combust. Sci. **26,** 417-458 (2000).

7. P. Glarborg, A. D. Jensen, and J. E. Johnsson, "Fuel nitrogen conversion in solid fuel fired systems," Prog. Energy Combust. Sci. **29,** 89-113 (2003).

8. N. Docquier and S. Candel, "Combustion control and sensors: a review," Prog. Energy Combust. Sci. **28,** 107-150 (2002).

9. V. Ebert, H. Teichert, P. Strauch, T. Kolb, H. Seifert, and J. Wolfrum, "Sensitive in situ detection of CO and O_2 in a rotary kiln-based hazardous waste incinerator using 760 nm and new 2.3 μm diode lasers," Proc. Combust. Inst. **30,** 1611-1618 (2005).

10. A. Khorsandi, U. Willer, L. Wondraczek, and W. Schade, "*In situ* and online monitoring of CO in an industrial glass furnace by mid-infrared difference-frequency generation laser spectroscopy," Appl. Opt. **43,** 6481-6486 (2004).

11. H. Teichert, T. Fernholz, and V. Ebert, "Simultaneous *in situ* measurement of

CO, H_2O, and gas temperatures in a full-sized coal-fired power plant by near-infrared diode lasers," Appl. Opt. **42,** 2043-2051 (2003).

12. E. Schlosser, T. Fernholz, H. Teichert, and V. Ebert, "In situ detection of potassium atoms in high-temperature coal-combustion systems using near-infrared-diode lasers," Spectrochim. Acta A **58,** 2347-2359 (2002).

13. E. Schlosser, J. Wolfrum, L. Hildebrandt, H. Seifert, B. Oser, and V. Ebert, "Diode laser based *in situ* detection of alkali atoms: development of a new method for determination of residence-time distribution in combustion plants," Appl. Phys. B **75,** 237-247 (2002).

14. M. G. Allen, B. L. Upschulte, D. M. Sonnenfroh, W. J. Kessler, and P. A. Mulhall, "Overview of diode laser measurements in large-scale test facilities," AIAA Paper 2000-2452 (2000).

15. W. J. Kessler, D. M. Sonnenfroh, B. L. Upschulte, and M. G. Allen, "Near-IR diode lasers for *in-situ* measurements of combustor and aeroengine emissions," paper AIAA 97-2706, presented at the *33rd AIAA/ASME/SAE/ASEE Joint Propulsion Conference*, Seattle, WA, 6-9 July 1997 (American Institute of Aeronautics and Astronautics, 555 West 57th Street, New York, 1997).

16. D. M. Sonnenfroh and M. G. Allen, "Absorption measurements of the second overtone band of NO in ambient and combustion gases with a 1.8-μm room-temperature diode laser," Appl. Optics **36**, 7970-7977 (1997).

17. R. M. Mihalcea, D. S. Baer, and R. K. Hanson, "A diode-laser absorption sensor system for combustion emission measurements," Meas. Sci. Technol. **9**, 327-338 (1998).

18. M. Snels, C. Corsi, F. D'Amato, M. De Rosa, and G. Modugno,"Pressure broadening in the second overtone of NO, measured with a near infrared DFB laser," Opt. Commun. **159**, 80-83 (1999).

19. D. B. Oh and A. C. Stanton, "Measurement of nitric oxide with an antimonide diode laser," Appl. Optics **36**, 3294-3297 (1997).

20. P. K. Falcone, R. K. Hanson, and C. H. Kruger, "Tunable diode laser absorption measurements of nitric oxide in combustion gases," Combust. Sci. Technol. **35**, 81-99 (1983).

21. D. D. Nelson, M. S. Zahniser, J. B. McManus, C. E. Kolb, and J. L. Jimenez, "A tunable diode laser system for the remote sensing of on-road vehicle emissions," Appl. Phys. B **67**, 433-441 (1998).

22. A. Mohamed, B. Rosier, D. Henry, Y. Louvet, and P. L. Varghese, "Tunable diode laser measurements on nitric oxide in a hypersonic wind tunnel," AIAA J. **34,** 494-499 (1996).

23. D. M. Sonnenfroh, W. T. Rawlins, M. G. Allen, C. Gmachl, F. Capasso, A. L. Hutchinson, D. L. Sivco, J. N. Baillargeon, and A. Y. Cho, "Application of balanced detection to absorption measurements of trace gases with room-

temperature, quasi-cw quantum-cascade lasers," Appl. Optics **40**, 812-820 (2001).

24. D. D. Nelson, J. H. Shorter, J. B. McManus, and M. S. Zahniser, "Sub-part-per-billion detection of nitric oxide in air using a thermoelectrically cooled mid-infrared quantum cascade laser spectrometer," Appl. Phys. B **75**, 343-350 (2002).

25. S. Wehe, M. Allen, L. Xiang, J. Jeffries, and R. Hanson, "NO and CO absorption measurements with a mid-IR quantum cascade laser for engine exhaust applications," paper AIAA 03-0588, presented at the *41st AIAA Aerospace Sciences Meeting and Exhibit*, Reno, NV, 6-9 January 2003 (American Institute of Aeronautics and Astronautics, 555 West 57th Street, New York, 2003).

26. G. Wysocki, A. A. Kosterev, and F. K. Tittel, "Spectroscopic trace-gas sensor with rapidly scanned wavelengths of a pulsed quantum cascade laser for in situ NO monitoring of industrial exhaust systems," Appl. Phys. B **80,** 617-625 (2005).

27. J. Luque and D. R. Crosley, "LIFBASE: Database and Spectral Simulation Program (Version 1.5)," SRI International Report MP 99-009 (SRI International, Menlo Park, Calif., 1999), www.sri.com/psd/lifbase.

28. L. S. Rothman, D. Jacquemart, A. Barbe, D. Chris Benner, M. Birk, L. R. Brown, M. R. Carleer, C. Chackerian Jr., K. Chance, L. H. Coudert, V. Dana, V. M. Devi, J.-M. Flaud, R. R. Gamache, A. Goldman, J.-M. Hartmann, K. W. Jucks, A. G. Maki, J.-Y. Mandin, S. T. Massie, J. Orphal, A. Perrin, C. P. Rinsland, M. A. H. Smith, J. Tennyson, R. N. Tolchenov, R. A. Toth, J. Vander Auwera, P. Varanasi,

G. Wagner, "The *HITRAN* 2004 molecular spectroscopic database," J. Quant. Spectrosc. Radiat. Transfer **96,** 139-204 (2005).

29. J. P. Koplow, D. A. V. Kliner, and L. Goldberg, "Development of a narrow-band, tunable, frequency-quadrupled diode laser for UV absorption spectroscopy," Appl. Opt. **37,** 3954-3960 (1998).

30. S. F. Hanna, R. Barron-Jimenez, T. N. Anderson, R. P. Lucht, J. A. Caton, and T. Walther, "Diode-laser-based ultraviolet absorption sensor for nitric oxide," Applied Phys. B **75,** 113-117 (2002).

31. T. N. Anderson, R. P. Lucht, R. Barron-Jimenez, S. F. Hanna, J. A. Caton, T. Walther, S. Roy, M. S. Brown, J. R. Gord, I. Critchley, and L. Flamand, "Combustion exhaust measurements of nitric oxide with an ultraviolet diode-laser-based absorption sensor," Appl. Opt. **44,** 1491-1502 (2005).

32. L. Hildebrandt, R. Knispel, S. Stry, J. R. Sacher, and F. Schael, "Antireflection-coated blue GaN laser diodes in an external cavity and Doppler-free indium absorption spectroscopy," Appl. Opt. **42,** 2110-2118 (2003).

33. H. Leinen, D. Glaessner, H. Metcalf, R. Wynands, D. Haubrich, and D. Meschede, "GaN blue diode lasers: a spectroscopist's view," Appl. Phys. B **70,** 567-571 (2000).

34. See http://www.sacher-laser.com.

35. J. Hult, I. S. Burns, and C. F. Kaminski, "Wide-bandwidth mode-hop-free tuning

of extended-cavity GaN diode lasers," Appl. Opt. **44,** 3675-3685 (2005).

36. U. Gustafsson, G. Somesfalean, J. Alnis, and S. Svanberg, "Frequency-modulation spectroscopy with blue diode lasers," Appl. Opt. **39,** 3774-3780 (2000).

37. H. Scheibner, S. Franke, S. Solyman, J. F. Behnke, C. Wilke, and A. Dinklage, "Laser absorption spectroscopy with a blue diode laser in an aluminum hollow cathode discharge," Rev. Sci. Instrum. **73,** 378-382 (2002).

38. O. M. Marago, B. Fazio, P. G. Gucciardi, and E. Arimondo, "Atomic gallium laser spectroscopy with violet/blue diode lasers," Appl. Phys. B **77,** 809-815 (2003).

39. T. N. Anderson, J. K. Magnuson, and R. P. Lucht, "Diode-laser-based sensor for ultraviolet absorption measurements of atomic mercury," Appl. Phys. B (in press).

40. S. Arumugam, "Nitrogen Oxides Emission Control Through Reburning With Biomass in Coal-Fired Power Plants," M.S. Thesis, Department of Mechanical Engineering, Texas A&M University, College Station, TX, December 2004.

41. K. Annamalai, B. Thien, and J. Sweeten, "Co-firing of coal and cattle feedlot biomass (FB) fuels. Part II. Performance results from 30 kW_t (100,000 BTU/h) laboratory scale boiler burner," Fuel **82,** 1183-1193 (2003).

42. S. Frazzitta, K. Annamalai, and J. Sweeten, "Performance of a burner with coal and coal-bio-solid fuel blends," J. Prop. Power **15,** 181-186 (1999).

43. K. Annamalai and J. M. Sweeten, "A Reburn System with Feedlot Biomass for

Maximum NOx Reduction in Power Plants," U.S. Patent #6,973,883, U.S. Patent Office, December 13, 2005.

44. R. P. Lucht, T. N. Anderson, S. Priyadarsan, S. Arumugam, R. Barron-Jimenez, J. A. Caton, and K. Annamalai, "Diode-laser-based sensor measurements of nitric oxide in particulate-laden combustion exhaust streams," Paper 14-2 in *Proceedings of the Twentieth Annual International Pittsburgh Coal Conference*, Pittsburgh, Pennsylvania, September 15-19, 2003.

45. T. R. Meyer, S. Roy, T. N. Anderson, J. D. Miller, V. R. Katta, R. P. Lucht, and J. R. Gord, "Measurements of OH mole fraction and temperature up to 20 kHz by using a diode-laser-based UV absorption sensor," Appl. Opt. **44,** 6729-6740 (2005).

46. S. T. Sanders, J. Wang, J. B. Jeffries, R. K. Hanson, "Diode-laser absorption sensor for line-of-sight gas temperature distributions," Appl. Opt. **40,** 4404-4415 (2001).

List of Figure Captions

Fig. 1. Comparison of line strengths for NO and H_2O at 296 K. Data for UV line strengths of NO are from Luque and Crosley,[27] and data for IR line strengths of NO and H_2O are from Rothman *et al.*[28] LineStrengthComparison.eps.

Fig. 2. Diagram of ECDL in the Littrow configuration with an AR-coated GaN laser diode. ECDLInternalDiagram.eps.

Fig. 3. A complete cycle of the waveforms generated with LabVIEW software to control the GaN ECDL. ECDLControlSignals.eps.

Fig. 4. Etalon signal recorded during a single scan of the ECDL wavelength, demonstrating the 90 GHz mode-hop-free tuning range with the new ECDL and control scheme. The free spectral range of the etalon is 2 GHz. ECDLTuningRange.eps.

Fig. 5. Schematic diagram of diode-laser-based sensor for NO measurements in coal-combustion exhaust. NOSensorDiagram-CoalLayout.eps.

Fig. 6. Schematic diagram of coal-fired boiler burner with reburn at Texas A&M University. CoalExhaustBurner.eps.

Fig. 7. Absorption spectra of nitric oxide acquired in coal-combustion exhaust using (a) the old ECDL and (b) the new ECDL. Both spectra were acquired in approximately 1 second. CoalSpectra-New+Old.eps.

Fig. 8. Distribution of NO mole fraction along the UV-beam path through the exhaust test section as measured with the electrochemical sensor for coal/biomass reburn at

Φ=1.0. The polynomial fit through the data is shown. NO mole fraction is assumed to be 0 ppm at the windows ($\pm$13.5 cm). NOExhaustDistribution.eps.

Fig. 9. Absorption spectrum of NO in the exhaust stream of the boiler burner at the same conditions as Fig. 8. The experimental spectrum was acquired in 5 seconds (40 Hz, 192 sweeps averaged). NOSpectrum-Biomass.eps

Fig. 10. Absorption spectrum of NO in the coal-combustion exhaust acquired in 0.2 seconds (40 Hz, 8 sweeps averaged) for coal/biomass reburn at Φ=1.0 without the air purge on the windows. NOSpectrum-8ptAvg-UVPower.eps.

Fig. 11. Summary of minimum NO mole fractions measured in the exhaust stream of the boiler burner with reburn for different fuel types and equivalence ratios. Mole fractions were measured *in situ* with the diode-laser sensor (TDLAS) and with extractive sampling and the EC sensor. Error bars represent the 10% uncertainty in diode-laser measurements. ReburnResultsSummary.eps

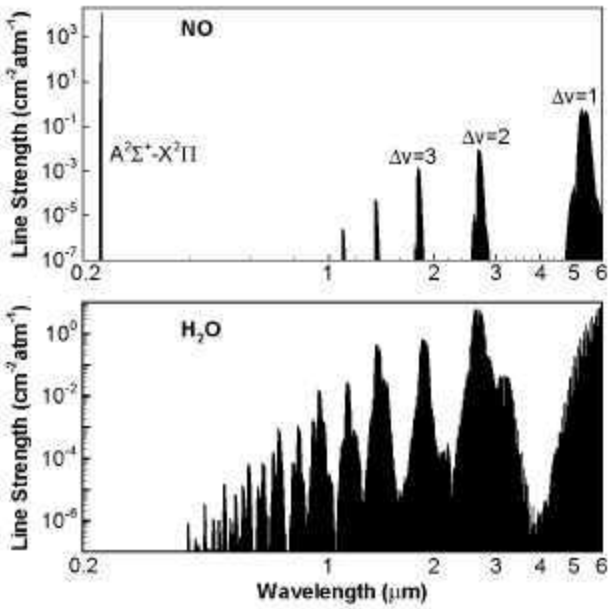

Fig. 1. Comparison of line strengths for NO and H_2O at 296 K. Data for UV line strengths of NO are from Luque and Crosley,[27] and data for IR line strengths of NO and H_2O are from Rothman *et al.*[28] LineStrengthComparison.eps.

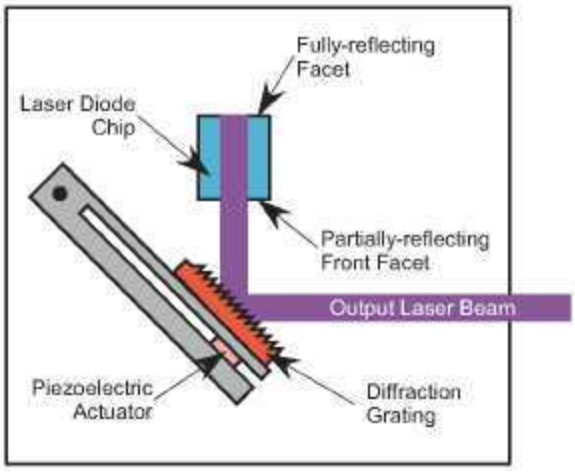

Fig. 2. Diagram of ECDL in the Littrow configuration with an AR-coated GaN laser diode. ECDLInternalDiagram.eps.

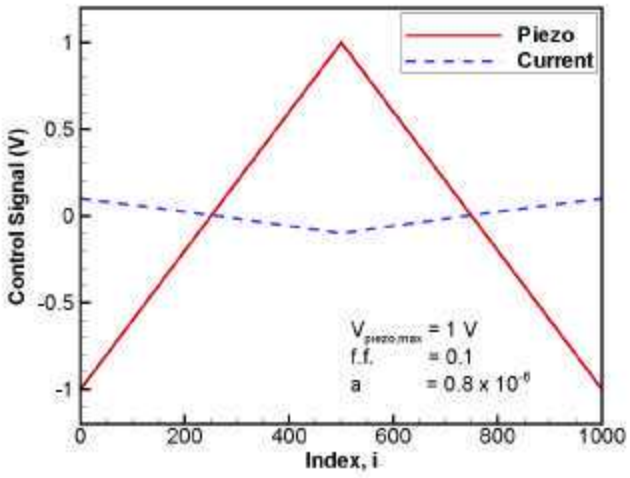

Fig. 3. A complete cycle of the waveforms generated with LabVIEW software to control the GaN ECDL. ECDLControlSignals.eps.

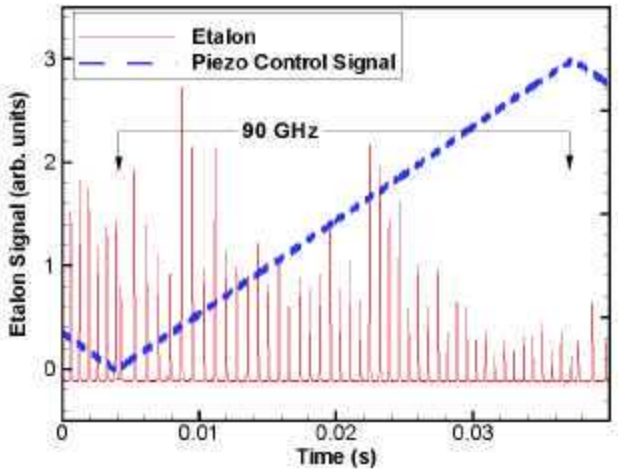

Fig. 4. Etalon signal recorded during a single scan of the ECDL wavelength, demonstrating the 90 GHz mode-hop-free tuning range with the new ECDL and control scheme. The free spectral range of the etalon is 2 GHz. ECDL-TuningRange.eps.

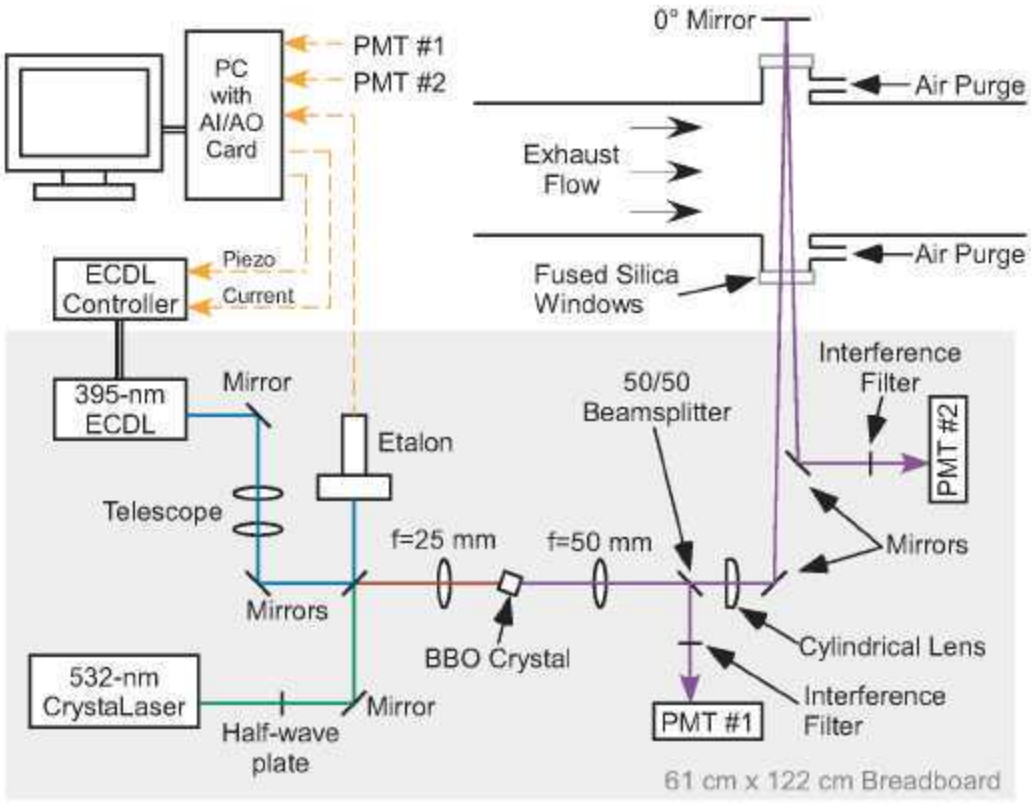

Fig. 5. Schematic diagram of diode-laser-based sensor for NO measurements in coal-combustion exhaust. *Note: Do not shrink to column width.* NOSensorDiagram-CoalLayout.eps.

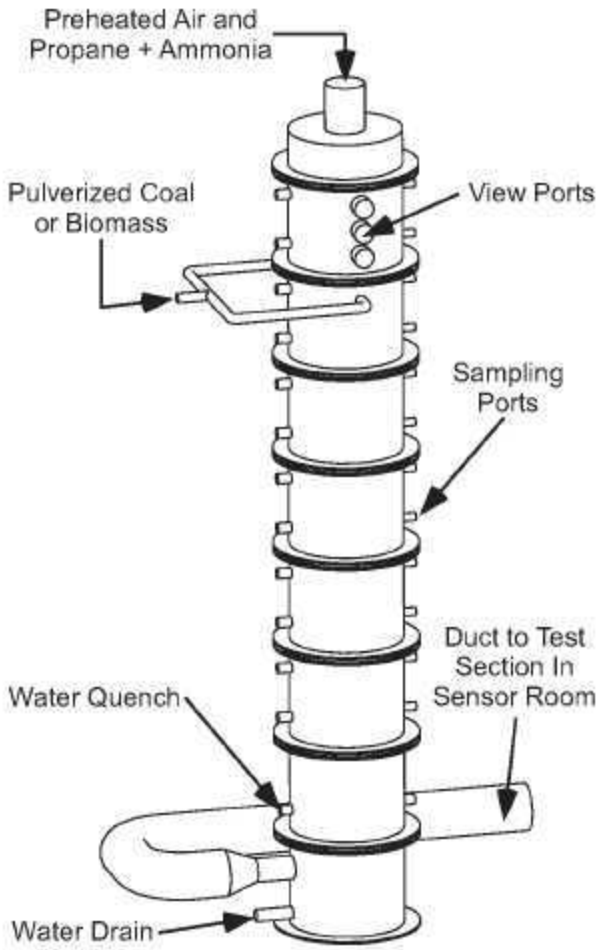

Fig. 6. Schematic diagram of coal-fired boiler burner with reburn at Texas A&M University. CoalExhaustBurner.eps.

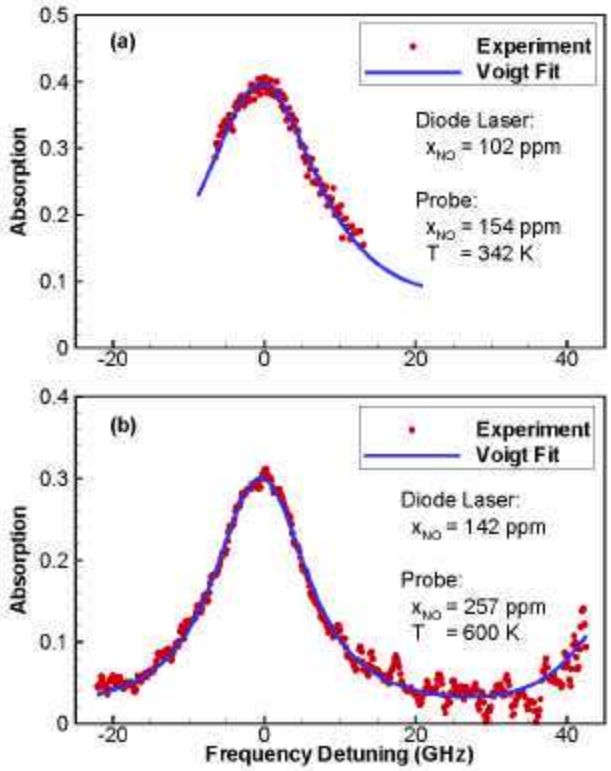

Fig. 7. Absorption spectra of nitric oxide acquired in coal-combustion exhaust using (a) the old ECDL and (b) the new ECDL. Both spectra were acquired in approximately 1 second. CoalSpectra-New+Old.eps.

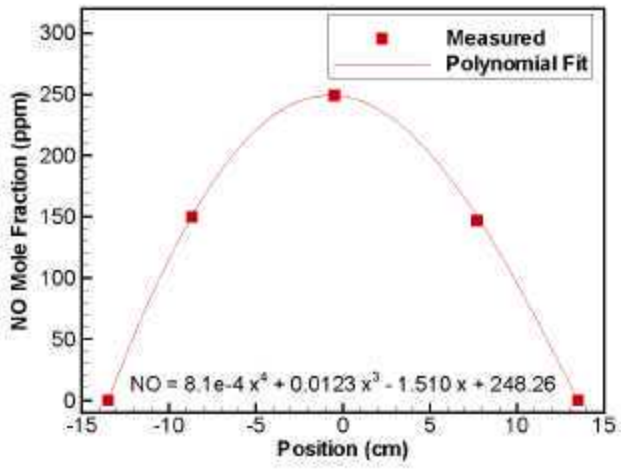

Fig. 8. Distribution of NO mole fraction along the UV-beam path through the exhaust test section as measured with the electrochemical sensor for coal/biomass reburn at Φ=1.0. The polynomial fit through the data is shown. NO mole fraction is assumed to be 0 ppm at the windows ($\pm$13.5 cm). NOExhaustDistribution.eps.

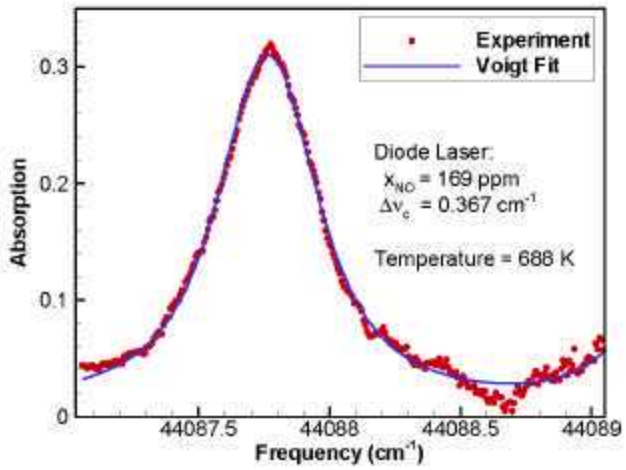

Fig. 9. Absorption spectrum of NO in the exhaust stream of the boiler burner at the same conditions as Fig. 8. The experimental spectrum was acquired in 5 seconds (40 Hz, 192 sweeps averaged). NOSpectrum-Biomass.eps

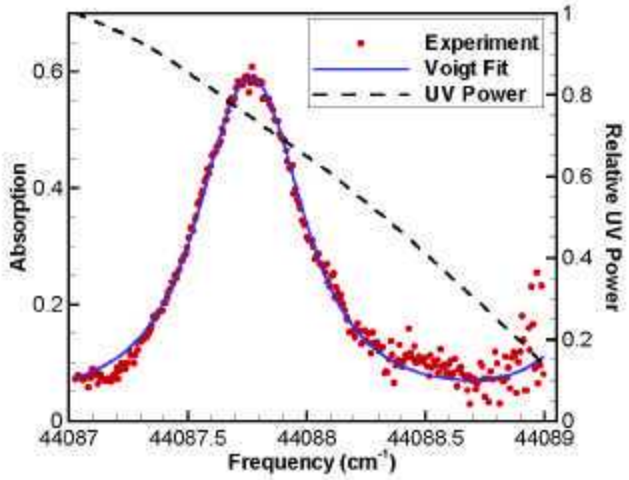

Fig. 10. Absorption spectrum of NO in the coal-combustion exhaust acquired in 0.2 seconds (40 Hz, 8 sweeps averaged) for coal/biomass reburn at Φ=1.0 without the air purge on the windows. NOSpectrum-8ptAvg-UVPower.eps.

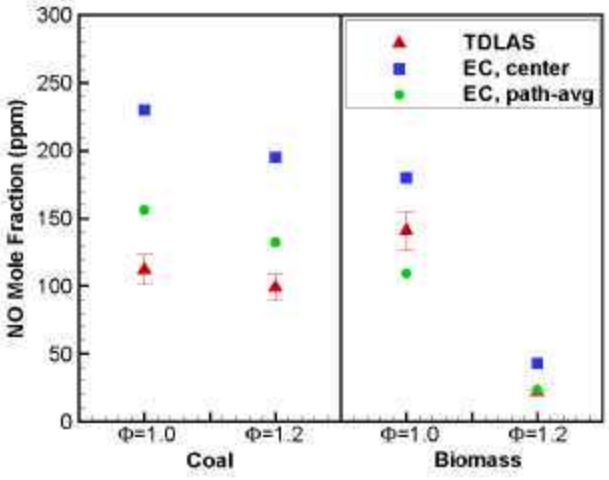

Fig. 11. Summary of minimum NO mole fractions measured in the exhaust stream of the boiler burner with reburn for different fuel types and equivalence ratios. Mole fractions were measured *in situ* with the diode-laser sensor (TDLAS) and with extractive sampling and the EC sensor. Error bars represent the 10% uncertainty in diode-laser measurements. ReburnResultsSummary.eps